

The influence of carrier layer material in ultrasonic particle manipulation devices

R. J. Townsend, M. Hill, N. R. Harris¹, D. Brennan¹, D. Wenn¹

School of Engineering Sciences, University of Southampton, SO17 1BJ, UK

¹School of Electronics and Computer Science, University of Southampton, SO17 1BJ, UK

Abstract: The use of acoustic radiation forces for the manipulation of particles, bacteria and cells is drawing increasing interest. Resonators using quarter-wavelength sized fluid chambers have been developed, where an acoustic pressure node is positioned near the reflector layer surface such that particles may be pushed close to or onto this surface. The thickness of the reflector layer has already been shown to greatly influence the performance of such resonators. These devices have applications in bio-sensing where a concentrate of particulates can be collected or particulates can be contacted with a sensor surface directly.

A coupling layer is usually incorporated into the device and is located between the transducer and fluid layer. The ability of this layer to act as an acoustic matching layer depends on its acoustic properties and thickness. Here, the performance of various carrier layer materials in a near quarter-wavelength device is investigated and compared using modelled and experimental data. Results indicate that where the carrier layer thickness is selected for optimum performance, the resonator performance is comparable for most high Q factor carrier layer materials. However, for some materials the performance of the resonator, is highly sensitive to the coupling layer thicknesses and in turn can constrain the flexibility of the acoustic design.

Key words: Acoustic radiation force, concentration, particles

A. Introduction

Ultrasonic particle manipulators typically have a multilayered structure to transmit acoustic energy from a piezo-electric transducer via a coupling layer into a fluid chamber where particles or cells are contained. Acoustic resonance of this structure generates acoustic radiation forces which is the mechanism used to manipulate particles within the fluid chamber to drive them to acoustic nodal planes [1].

These systems can be realised on a macro or micro-fluidic scale and are being developed for use in bio-sensing and life science applications. A typical example are quarter-wavelength resonators ($\lambda/4$ depth fluid chambers) where particles are forced up to the reflector surface [2],[3]. Compared to $n\lambda/2$ depth chambers, such as half-wavelength chambers, quarter-wavelength devices are less energy efficient because of the reliance on a reflector layer resonance where much of the acoustic

energy is dissipated. The design of these systems therefore presents an interesting challenge and it has already been shown by [3] that the reflector layer thickness has a significant influence on performance.

This paper is concerned with the coupling layer material which is located between the transducer and fluid chamber. Various materials have been used for the coupling layer, for example, an acrylic wedge has been used as a coupling element in [4] compared to the more usual higher impedance materials such as stainless steel. Ease of manufacture or biocompatibility also influence material choice, for example, micro-fabricated silicon devices have been successfully demonstrated by [5]. As well as the dimensions of the various acoustic components and the frequency used to excite the system, it is assumed that the coupling layer material also influences the acoustic energy density and the maximum radiation force experienced by a particle. This is highly relevant to quarter-wavelength systems as the success of a resonator typically relies on maximising the acoustic energy density, thus lowering the power and voltage required and resulting in efficient operation. Here we investigate the coupling layer material and its effect on the acoustic energy within the fluid layer. Experimental measurements of acoustic energy density are used to refine a model which is then used to provide a comparison between the materials considered.

B. Acoustic Simulations

An acoustic impedance transfer model was used to predict the 1-dimensional acoustic behaviour of the resonator [6]. This uses an equivalent circuit model to describe the system and is able to predict the acoustic pressure and velocity fields through the various layers of the device. This in turn provides an estimate of the acoustic energy density and radiation force acting on a particle. In this study the role of the model is:

- (1) Determine initial experimental design
- (2) Simulate the behaviour of other designs.

B.1. Initial experimental design

Initial simulations were used to design a near quarter-wavelength resonator operating around 2MHz. The typical acoustic pressure profile within such a device is shown in Fig.1 where a half-wavelength resonance is seen in the reflector layer above the fluid chamber. This resonance imposes a node at the fluid/reflector boundary and for certain fluid depths will result in a quarter-wavelength "resonance" in the fluid layer. The effect of

this mode forces suspended particles up to this surface.

For the experimental devices a transducer with a resonance close to the operating frequency of the assembled transducer was used (Ferroperm PZ26, 1mm thick). To give comparable acoustic pressure profiles in the fluid layer, the model was used to select coupling layer and fluid layer thickness dimensions. In each case the fluid layer thickness was chosen to be 0.18mm and coupling layer thicknesses of 1.0, 1.4, and 1.2 were selected for brass, aluminium and Macor, respectively. Table 1 contains the measured thickness dimensions and acoustic properties used in the initial modelling

B.2. Simulation of other designs

Measurements of acoustic energy density in the fabricated resonators are used to revise the acoustic parameters used by the model. The revised model is then used to illustrate the influence of the coupling layer material upon the design and performance of the resonator by simulating a greater number of resonator designs.

C. Experimental Device

As indicated in Fig.1, the experimental device is a multilayered construction and uses a modular approach such that the same reflector layer can be used with each coupling layer sample. A micro-mill (Datron) is used to mill a plate of the coupling layer material to the combine thickness of the fluid and coupling layers. Then within the same machining step, a rectangular recess is machined into the plate to a depth of 0.18mm to form the fluid chamber. The fluid chamber and the thickness of the coupling layer beneath the fluid chamber are both measured before the transducer is assembled onto the sample and are also listed in Table 1. It can be seen that the machining processes results in a thickness error of up to 0.08mm in the matching layer, but only 0.01mm in the fluid layer. Although stainless steel has had notable use in similar devices as in [3] and would ideally feature in this study, the milling of this material has proved difficult.

The mill is also used to fabricate a mould to form a silicone rubber gasket. This seals the fluid chamber, but as it is also used to create the walls of the fluid chamber as it is thought to limit acoustic enclosure modes by increasing lateral damping.

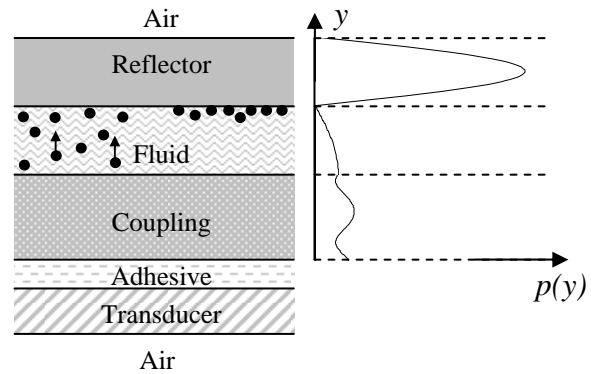


Fig.1. Schematic of acoustic pressure field within multi-layered resonator illustrating movement of particles up to the reflector surface.

D. Experimental Results

In the case of Macor, the characteristics of this design are plotted in Fig.2 showing two resonances around 2MHz. The lower frequency resonance ~ 2.05MHz is associated with the reflector layer, i.e. similar to the pressure profile shown in Fig.1, whereas the resonance ~2.2 to 2.3MHz is caused by the coupling between the transducer and coupling layer. The modelled electrical impedance shows a good comparison with the measured data and demonstrates that resonant modes and their approximate frequency can be predicted with confidence.

Acoustic energy density measurements are taken between 1.96 and 2.1MHz at 10kHz intervals. These measurements are made by levitating a polystyrene particle and recording the threshold voltage where the particles begins to sediment, similar to the method described by [3]. For the particles, fluid (water) and frequency used, this threshold voltage corresponds to a pressure amplitude of 33kPa. During experiments, the position of the node is difficult to measure accurately but is reasonably consistent with predictions of the pressure profile such as that shown in Fig.2 (b). As the acoustic pressure amplitude is proportional to the transducer voltage, the pressure amplitude P_0 resulting from a 10Vpkpk voltage is recorded and converted to an energy density measurement using (1):

$$\langle \bar{\epsilon} \rangle = \frac{1}{4} P_0^2 \beta_w, \quad (1)$$

where $\langle \bar{\epsilon} \rangle$ is the acoustic energy density and β_w is the bulk modulus of water, with the results presented in Fig.3.

Table 1. Dimensions of experimental samples. Properties of materials taken from [7].

Coupling layer material	Coupling layer thickness (mm)		Fluid layer thickness (mm)		Density (kg/m ³)	Sonic velocity (m/s)	Acoustic impedance (MRayl)
	Design	Measured	Design	Measured			
Brass	1.00	1.08	0.18	0.17	8640	4700	40.6
Aluminium	1.40	1.42	0.18	0.175	2700	6420	17.3
Macor	1.20	1.17	0.18	0.19	2540	5510	14.0

These plots show that the acoustic energy density peaks at a certain frequencies where resonant modes are

encountered. Predicted energy density is also shown, where the input parameters to the model have been modified to improve the match with both impedance and

energy density measurements. Notably the quality (loss) factors have been adjusted to 300, 100 and 100 for brass, aluminium and Macor, respectively. Similarly, the quality factors in the fluid and reflector are low at ~ 50 and ~ 100 , respectively.

In the case of brass, two peaks can be seen although the model suggests that the peak around 1.98MHz is a combined transducer and coupling layer resonance. This mode appears to be particularly energetic and may be reinforced, for example, by structural modes.

E. Modelled Results

To compare each material more directly, the model is used to simulate the effect of coupling layer thickness whilst applying identical reflector and fluid layer properties. Fig.4 shows the predicted peak energy density for a range of coupling layer thicknesses as a fraction of wavelength (t_m/λ) and where the transducer voltage is a constant 10Vpkpk. Note that Fig.4 is generated by locating the frequency at which the quarter-wavelength mode (reflector resonance) occurs and omits any other resonant modes close to this frequency. It therefore does not include the high energy resonance seen at 1.98MHz in the experimental results for the brass coupling material.

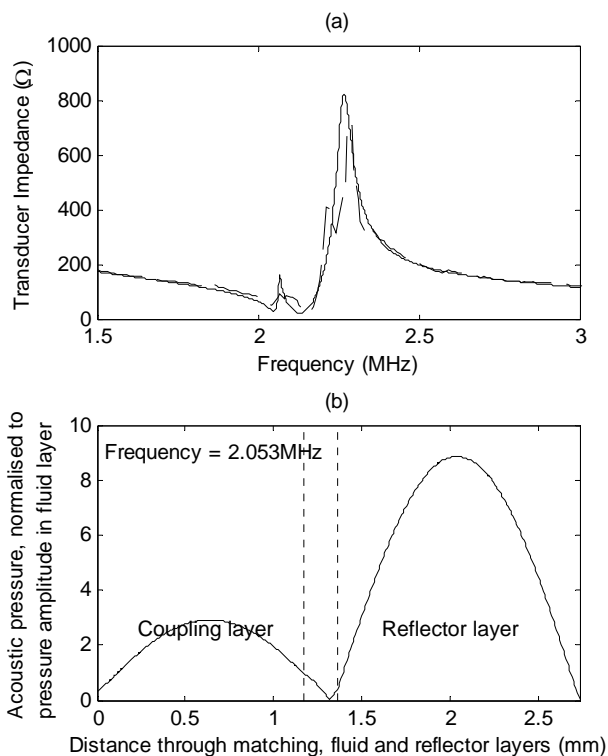


Fig.2. Measured (dashed) and predicted (solid) electrical impedance (a), and predicted acoustic pressure profile (b) within the coupling, fluid and reflector layers at the near-quarter-wavelength resonance.

In general, the energy density is comparable for the materials considered, although the material does have a limited impact in the maximum energy density achievable. Peaks suggest that for all the materials tested a coupling layer thickness of just under $n \cdot t_m / 2\lambda$ ($n = 1, 2$

only shown) results in a higher acoustic energy. The trade-off in this case is that the acoustic node moves away from the surface and further into the fluid layer at these dimensions. As the transducer is operating close to a half-wavelength, the peaks also coincide with a wavelength resonance in the transducer and coupling layer combined where if this structure were isolated from the fluid and reflector would have a pressure node located on the coupling layer surface. The close proximity of this coupled resonance to the quarter-wavelength mode may therefore be responsible for the change in energy density and movement of the node towards the coupling layer surface. Also, for an increase in n the energy density decreases, likely due to greater losses within a progressively thicker coupling layer.

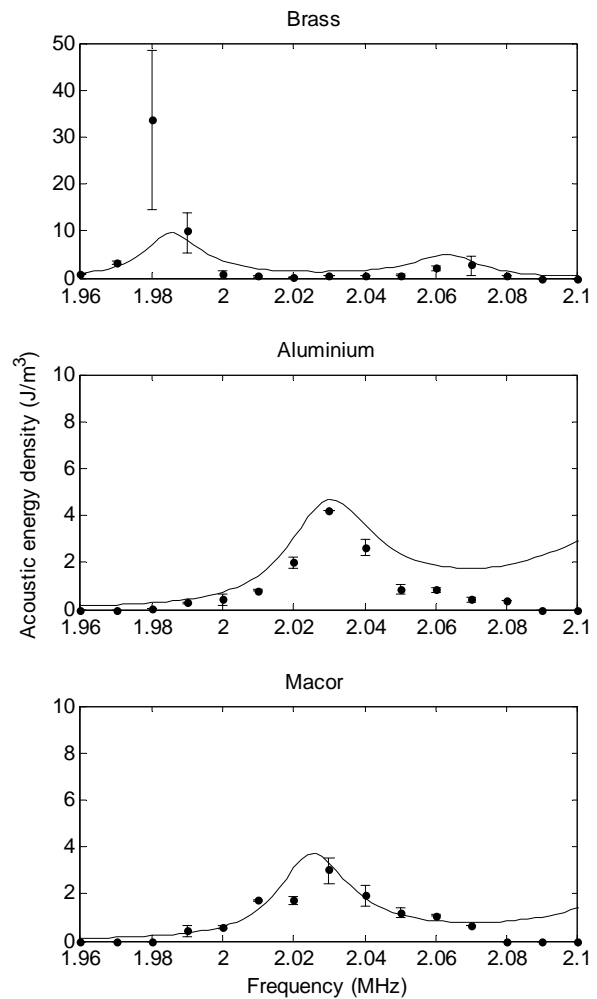


Fig.3. Comparison between measured and modelled acoustic energy density.

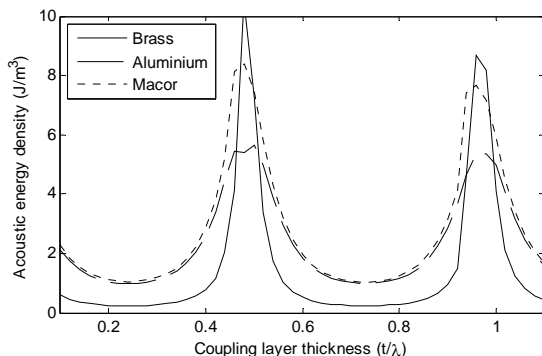


Fig.4. Predicted peak acoustic energy density in the fluid layer for a range of coupling layer thicknesses.

Another interesting feature is in between these high energy regions where the lower impedance materials provide better acoustic matching than the high impedance brass. This suggests that a more dimensionally robust design may be achieved using lower impedance materials, especially where a long design process needs to be avoided. Further experimental work using designs in these less energetic regions would be required to support this theory. Also, on-going work suggests that the losses in the reflector layer have a significant effect on the energy density and justifies further study.

F. Conclusions

It has been shown that the behaviour of ultrasonic resonators for the generation of quarter-wavelength modes can be more fully understood based on a comparison of modelled and experimental data. We show that using experimental data to refine the simulation input parameters it is possible to predict the acoustic energy density well within the correct order of magnitude. This is important, for example, for bio-sensing applications where the location of the pressure node and strength of the field influences significantly the feasibility of such devices. The choice of material used to couple between the transducer and fluid manipulation chamber determines to a limited extent the maximum energy density achievable, although coupling layer thickness appears to have a greater impact. This study has therefore demonstrated that an increasing range of materials can be considered for ultrasonic resonator designs which increases the versatility of these devices in terms of their applications and fabrication methods.

G. Literature

- [1] M. Gröschl, "Ultrasonic separation of suspended particles - Part I: Fundamentals," *Acustica*, vol. 84(3), pp. 432-447, 1998.
- [2] J.J. Hawkes, M.J. Long, W.T. Coakley, and M.B. McDonnell, "Ultrasonic deposition of cells on a surface," *Biosensors & Bioelectronics*, vol. 19(9), pp. 1021-1028, 2004.
- [3] S.P. Martin, R.J. Townsend, L.A. Kuznetsova, K.A.J. Borthwick, M. Hill, M.B. McDonnell, and W.T. Coakley, "Spore and micro-particle capture on an immunosensor surface in an ultrasound standing wave system," *Bio-*

sensors and Bioelectronics, vol. 21(5), pp. 758-767, 2005.

- [4] M. Wiklund, C. Günther, R. Lemor, M. Jäger, F. G., and H.M. Hertz, "Ultrasonic standing wave manipulation technology integrated into a dielectrophoretic chip," *Lab on a Chip*, vol. 6(12), pp. 1537-1544, 2006.
- [5] N.R. Harris, M. Hill, S.P. Beeby, Y. Shen, N.M. White, J.J. Hawkes, and W.T. Coakley, "A Silicon Microfluidic Ultrasonic Separator," *Sensors and Actuators B*, vol. 95(1-3), pp. 425-434, 2003.
- [6] M. Hill, Y. Shen, and J.J. Hawkes, "Modelling of layered resonators for ultrasonic separation.,", *Ultrasonics*, vol. 40, pp. 385-392, 2002.
- [7] *Onda Coporation acoustic material tables*. Web page accessed March 2007:
http://www.ondacorp.com/tecref_acoustictable.html.